

DIELECTRIC RELAXATION AND AC CONDUCTIVITY OF Au/ (7% CdTe:PVA) /n-Si MPS STRUCTURES AT LOW FREQUENCIES

I.M. AFANDIYEVA¹, E.R. BAKHTIYARLI², C.G. AKHUNDOV¹

¹*Baku State University, Institute for Physical Problems, Baku, Azerbaijan*

²*Baku State University, Department of Physics, Baku, Azerbaijan*
I_afandiyeva@yahoo.com, elvinb18104@sabah.edu.az

In this work, we investigate the electrical and dielectric properties of a Au/7%CdTe-doped:PVA/n-Si hybrid structure by analyzing the capacitance–voltage (C–V) and conductance–voltage (G/ω–V) characteristics over a frequency range of 10 kHz and 200 kHz at room temperature. From these measurements, key dielectric parameters such as the real (ϵ') and imaginary (ϵ'') parts of the permittivity, as well as the frequency-dependent AC conductivity (σ_{ac}), were extracted within the applied voltage interval of 1.0 V to 1.2 V. The experimental results reveal a clear decrease in ϵ' and ϵ'' with increasing frequency, consistent with interfacial polarization and dielectric relaxation mechanisms typical of heterogeneous polymer–semiconductor systems. Notably, the AC conductivity exhibited a non-monotonic profile with distinct relaxation peaks, suggesting multiple transport mechanisms governed by interface states and CdTe-related trap centers. A representative numerical value of σ_{ac} reached approximately 5.5×10^{-8} S/cm at low frequencies under 1.2 V bias. These findings highlight the strong influence of CdTe doping on the polarization dynamics and field-dependent conduction behavior of the hybrid junction. Full interpretation of the electrical response and conduction mechanisms is provided in the conclusion.

Keywords: CdTe-doped PVA, metal–polymer–semiconductor (MPS) structure, dielectric properties, AC conductivity, interfacial polarization, impedance spectroscopy.

DOI: 10.70784/azip.1.2026127

INTRODUCTION

Introducing an insulating layer between a metal and a semiconductor transforms the traditional metal–semiconductor (MS) contact into a metal–insulator–semiconductor (MIS) structure, effectively altering its electrical characteristics. Such interlayers are known for their ability to polarize under external electric or magnetic fields, providing additional modulation in device performance. Although oxides like SiO₂ and SnO₂ are widely used due to their stability and ease of growth on semiconductor surfaces, they suffer from drawbacks such as increased leakage currents and insufficient passivation of interface defects or surface states (N_{ss}) [1-4]. These interface states, situated between the semiconductor and the insulating film, typically possess energy levels spanning the bandgap (E_g) and can act as dynamic charge trapping or recombination centers depending on their occupancy and external stimuli. Non-ideal behaviors often emerge in C–V and G/ω–V characteristics as a result of these interface states and polarization effects. At lower and intermediate frequencies, the period of the AC signal ($T = 1/2\pi f$) becomes longer than the time constant (τ) of the traps, allowing carriers to interact more effectively with the field. Under such conditions, both interface-state charging and interfacial dipole reorientation contribute significantly to the device response, manifesting as elevated capacitance and conductance values, particularly in the depletion region. Conversely, as the frequency increases, the ability of these traps to respond diminishes, resulting in their minimal contribution to the overall dielectric behavior [5-8]. Efforts to address these limitations have increasingly turned to advanced materials that replace traditional insulators with organic or nanocomposite interfacial layers [2,4]. Recent developments have demonstrated that polymer-based dielectrics doped

with nanoparticles or metal oxides can offer superior electrical performance by passivating surface states more effectively and enhancing dielectric constants. Conventional polymers like polyvinyl alcohol (PVA) and polyvinylpyrrolidone (PVP) are frequently selected due to their processability, solubility, and functional group compatibility. However, these polymers alone exhibit low conductivity and modest dielectric response, which limits their standalone application. Enhancing the dielectric performance of polymers can be achieved by doping them with nanoscale semiconductors or metal oxides [8-13]. Materials such as ZnO, MnO, Co, CdTe, and graphene have shown promise in this role, significantly improving charge storage, interfacial polarization, and trap-state modulation. In particular, cadmium telluride (CdTe), a II–VI compound semiconductor, is highly attractive due to its direct bandgap of approximately 1.45 eV, high absorption coefficient ($>10^4$ cm⁻¹), excellent carrier mobility (~ 1040 cm²/V·s), and long-term thermal and chemical stability. These features make it ideal for integration into polymer matrices, especially for optoelectronic and dielectric applications [13-15]. Embedding CdTe nanoparticles within a PVA host matrix forms a hybrid dielectric layer capable of improving both polarization behavior and interface charge dynamics. PVA's semicrystalline nature, combined with its high thermal resistance, water solubility, and tunable dielectric profile, makes it a suitable platform for semiconductor–polymer integration. The resulting composite interlayer offers improved interface quality and dielectric response, making it a promising candidate for advanced MIS-type Schottky devices [15-19]. In this work, we carried out a comprehensive investigation into the electrical and dielectric characteristics of a Au/7%CdTe:PVA/n-Si hybrid structure. Measurements of capacitance (C–V), conductance (G/ω–V), real and imaginary dielectric

constants (ϵ' and ϵ''), and AC conductivity (σ_{ac}) were performed at room temperature over a forward bias voltage range of 1.0–1.2 V and at fixed frequencies of 10 kHz and 200 kHz. This study aims to clarify the role of CdTe-doped PVA as an interfacial layer in modifying the dielectric behavior, interface-state dynamics, and frequency-dependent electrical response of the heterojunction device.

EXPERIMENTAL DETAILS

In the present study, a metal–polymer–semiconductor (MPS) structure with the configuration Au/(Ni:PVP)/n-Si was fabricated on n-type silicon substrates. Preparation of the n-Si surface began with ultrasonic cleaning in a sequence of chemical acid and deionized water mixtures to remove organic and inorganic contaminants. Following this, the substrates were thoroughly rinsed with deionized water and subsequently dried using high-purity nitrogen gas to ensure a clean and moisture-free surface. Formation of the ohmic back contact was achieved by depositing a 150 nm-thick layer of high-purity aluminum onto the entire rear surface of the n-Si substrate, followed by a rapid thermal annealing process at 500 °C for 5 minutes. This step ensured good electrical contact and minimized contact resistance. To prepare the interfacial

dielectric layer, a nanocomposite CdTe:PVA solution was formulated by dispersing 10 mg of CdTe nanocrystals into 5 mL of a 0.07% aqueous PVA solution. This mixture was homogenized and then applied onto the front surface of the silicon wafer using the spin-coating technique, ensuring a uniform and thin polymer–nanoparticle film. Top Schottky contacts were created by thermally evaporating 150 nm-thick circular Au electrodes onto the CdTe:PVA-coated surface under high vacuum. This completed the formation of the MPS diode structure. Electrical characterization of the fabricated devices was carried out at room temperature using an HP4192A impedance analyzer. Capacitance–voltage (C–V) and conductance–voltage (G/ω–V) measurements were performed across a range of applied biases and at selected frequencies to extract dielectric parameters and analyze interfacial behavior.

RESULTS AND DISCUSSIONS

The frequency-dependent admittance technique, which including a set of capacitance/conductance (C/G–V) measurements, is generally utilized to calculate the real/ imaginary components of complex dielectrics, can be calculated with following formulas.

$$\epsilon^*(\omega) = \epsilon'(\omega) - j\epsilon'' = \left(\frac{C_m d_i}{A\epsilon_0}\right) - j\left(\frac{G_m d_i}{\omega A\epsilon_0}\right) = C_m/C_0 - j(G_m/\omega C_0) \quad (1)$$

The real part of the dielectric constant (ϵ') exhibits a strong dispersion in the low-frequency region, gradually declining as the frequency increases as shown in Fig 1 [16,19-21]. This frequency-dependent behavior can be attributed to interfacial polarization, particularly of the Maxwell–Wagner type, which is highly sensitive to the heterogeneous structure introduced by the CdTe:PVA layer [22-24]. At low frequencies, charge carriers have sufficient time to accumulate at the interfaces between CdTe quantum dots and the surrounding polymer matrix, as well as at the dielectric/semiconductor junction, leading to enhanced ϵ' values. However, as the frequency increases, the inability of dipoles and space charges to follow the rapidly alternating field results in a sharp decline of ϵ' , indicating a relaxation process where the dielectric response becomes more electronic and less orientational. The influence of voltage on ϵ' is equally notable. Increasing the applied forward bias from 1.0 V to 1.2 V leads to a consistent rise in ϵ' across the frequency spectrum [5,23-25]. This enhancement suggests an increased participation of space charge regions and interfacial states under higher electric fields, particularly those localized at the CdTe/PVA–Si interface and within the bulk of the CdTe:PVA composite itself. CdTe, being a direct bandgap II–VI semiconductor with high polarizability and significant dielectric constant, introduces deep and shallow trap centers when embedded in the polymeric host. These localized states can trap and release carriers depending

on the applied field, thus dynamically contributing to polarization processes. At a doping concentration of 7% CdTe by weight, the nanoparticle loading appears to be sufficient to form continuous or semi-continuous paths for polarization and limited conduction without reaching percolation. Below this threshold, dielectric enhancement is mainly driven by dipolar and interfacial contributions rather than direct carrier hopping between neighboring particles. This sub-threshold regime allows the dielectric properties to be tuned without introducing excessive leakage or conduction losses [24-26].

In the ϵ'' –f–V behavior as illustrating in Fig 2, the imaginary part of the dielectric constant shows a steep decline with increasing frequency, especially prominent in the low-frequency regime. This is characteristic of dielectric losses due to both conductive and relaxational processes. At low frequencies, the loss is dominated by space charge polarization and electrode effects, again amplified by the presence of CdTe - induced traps and heterojunction interfaces [2,17-20,24]. These losses decrease sharply with frequency, consistent with the reduction in charge carrier response time. Interestingly, the ϵ'' values show only slight sensitivity to applied voltage in the mid- to high-frequency range, suggesting that while voltage enhances polarization (as seen in ϵ'), it has a more subdued effect on loss mechanisms once the interface states become saturated or carriers are delocalized.

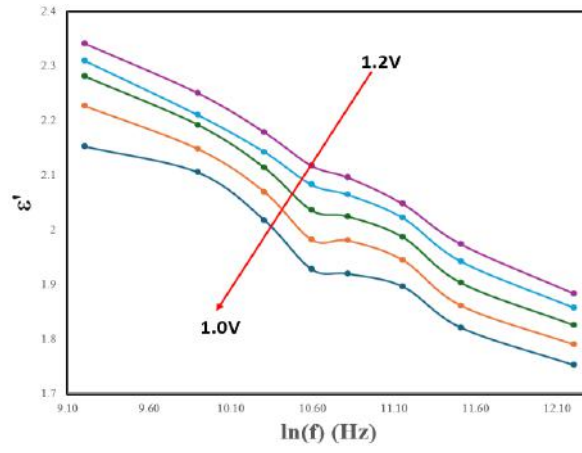


Fig 1. ϵ' - $\ln(f)$ graphic between 10kHz and 200kHz at 1V-1.2V voltage interval for Au/ (7% CdTe:PVA) /n-Si MPS

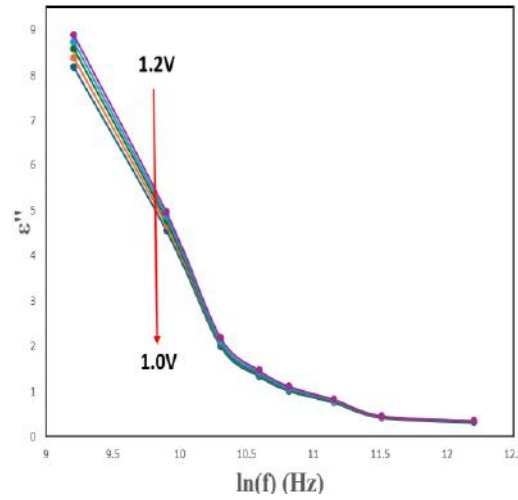


Fig 2. ϵ'' - $\ln(f)$ graphic between 10kHz and 200kHz at 1V-1.2V voltage interval for Au/ (7% CdTe:PVA) /n-Si MPS

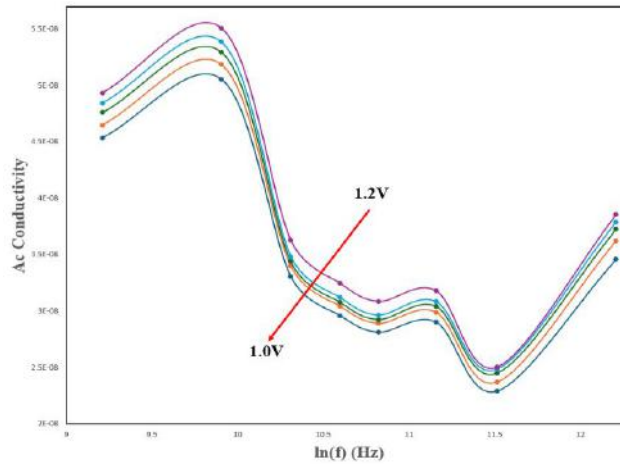


Fig 3. AC conductivity - $\ln(f)$ graphic between 10kHz and 200kHz at 1V-1.2V voltage interval Au/ (7% CdTe:PVA) /n-Si MPS

The AC conductivity spectrum, evaluating with following formula (2), exhibits a non-monotonic profile with characteristic peaks and depressions, reflecting complex dynamic mechanisms that govern charge mobility and polarization in the hybrid structure.

$$\sigma_{ac}(\omega) = \omega C(\tan\delta) \left(\frac{d_i}{A}\right) = 2\pi f \epsilon_0 \epsilon'' \quad (2)$$

At low frequencies, the conductivity increases gradually with frequency, consistent with enhanced

interfacial polarization and space charge contribution. In this region, the polymer matrix, modified by CdTe nanoparticle inclusion, facilitates charge accumulation at interfaces and localized hopping between trapping sites, which are enhanced under the influence of the external field. The rise in conductivity is attributed to Maxwell–Wagner-type interfacial polarization [13-18,22]. As frequency increases toward the mid-region of the plot, a distinct peak is observed around $\ln(f) \approx$

10.3 showing in Fig 3. Interestingly, at higher frequencies, the conductivity shows a secondary increase beginning around $\ln(f) \approx 11.5$, which may correspond to short-range or tunneling-type carrier motion. In this high-frequency regime, electronic polarization and localized charge carrier displacement become dominant. The behavior reflects the onset of a second conduction mechanism less reliant on dipolar reorientation and more governed by the intrinsic electrical properties of the composite material [11-16,26].

The decrease in ac conductivity in the frequency range of 20kHz and 50kHz and corresponds to the dependence according to the Drude model [27,28].

$$\sigma_{ac} = \sigma_{dc} \frac{1}{1+(\omega\tau)^2} \quad (3)$$

where $\omega = 2\pi f$ is the angular frequency, τ is the electron quasi-momentum relaxation time, and σ_{dc} is the dc-conductivity. The model satisfactorily describes the dependence of conductivity on frequency for metals and heavily doped semiconductors.

CONCLUSION

This study explored the electrical and dielectric behavior of the Au/7%CdTe:PVA/n-Si heterojunction through C–V and G/ω–V measurements conducted at room temperature over a forward bias range of 1.0–

1.2 V and at fixed frequencies of 10 kHz and 200 kHz. From these measurements, ϵ' , ϵ'' , and AC conductivity (σ_{ac}) were extracted to understand the polarization and transport mechanisms in the hybrid structure. ϵ' showed strong frequency dispersion, decreasing from ~2.35 to 1.75 as frequency increased, consistent with Maxwell–Wagner-type interfacial polarization. ϵ'' also decreased sharply with frequency, indicating that dielectric losses were dominated by space charge and dipolar relaxation at low frequencies. The AC conductivity spectrum revealed a clear peak near $\ln(f) \approx 10.3$, indicating a transition from interfacial polarization to hopping or localized conduction mechanisms. At higher frequencies, σ_{ac} increased again, suggesting short-range or tunneling transport. A maximum σ_{ac} value of $\sim 5.5 \times 10^{-8}$ S/cm was observed under 1.2 V at low frequency. The inclusion of 7% CdTe nanoparticles in the PVA matrix played a critical role in enhancing polarization and introducing field-sensitive trap states. This allowed for a well-controlled dielectric response and tunable conductivity. The results confirm that this hybrid structure supports voltage- and frequency-dependent dielectric relaxation and conduction, making it suitable for applications in sensors, memory devices, and tunable capacitive systems. The dependence of conductivity on frequency in the frequency range corresponds to the Drude model.

-
- [1] Ö. Berkün, M. Ulusoy, Ş. Altındal, B. Avar. On frequency and voltage dependent physical characteristics and interface states characterization of the metal semiconductor (MS) structures with (Ti:DLC) interlayer, *Physica B: Condensed Matter* 666, 415099, 2023. <https://doi.org/10.1016/j.physb.2023.415099>
- [2] M. Ulusoy, Y. Badali, G. Pirgholi-Givi, Y. Azizian-Kalandaragh, Ş. Altındal. The capacitance/conductance and surface state intensity characteristics of the Schottky structures with ruthenium dioxide-doped organic polymer interface, *Synthetic Metals* 292, 117243, 2023. <https://doi.org/10.1016/j.synthmet.2022.117243>
- [3] Y. Şafak Asar, Ö. Sevgili, Ş. Altındal. Investigation of dielectric relaxation and ac conductivity in Au/(carbon nanosheet-PVP composite)/n-Si capacitors using impedance measurements, *J. Mater. Sci. Mater. Elect.* 34, 893, 2023. <https://doi.org/10.1007/s10854-023-10320-1>
- [4] D. Ata, S. Altındal Yerişkin, A. Tataroğlu, M. Balbaşı. Analysis of admittance measurements of Al/Gr-PVA/p-Si (MPS) structure, *Journal of Physics and Chemistry of Solids* 169, 110861 2022. <https://doi.org/10.1016/j.jpcc.2022.110861>
- [5] G. Kandhol, H. Wadhwa, S. Chand, S. Mahendia, S. Kumar. Study of dielectric relaxation behavior of composites of Poly (vinylalcohol) (PVA) and Reduced graphene oxide (RGO), *Vacuum* 160, 384-393, 2019. <https://doi.org/10.1016/j.vacuum.2018.11.051>
- [6] S. Tewari, A. Bhattacharjee, P.P. Sahay. Structural, dielectric, and electrical studies on thermally evaporated CdTe thin films, *J. Mater. Sci.* 44, 534–540, 2009. <https://doi.org/10.1007/s10853-008-3088-x>
- [7] G. Fussell, J. Thomas, J. Scanlon, A. Lowman, M. Marcolongo. The effect of protein-free versus protein-containing medium on the mechanical properties and uptake of ions of PVA/PVP hydrogels, *J. Biomater. Sci.* 16, 489–503 (2005) <https://doi.org/10.1163/1568562053700219>
- [8] H. Bouaamlat, N. Hadi, N. Belghiti, H. Sadki, M. N. Bennani, F. Abdi, T. Lamcharfi, M. Bouachrine, M. Abarkan. Dielectric Properties, AC Conductivity, and Electric Modulus Analysis of Bulk Ethylcarbazole-Terphenyl. *Hindawi Advances in Materials Science and Engineering*, 8689150 1-8 (2020) <https://doi.org/10.1155/2020/8689150>
- [9] A. Feizollahi Vahid, S. Alptekin, N. Basman, M. Ulusoy, Y. Şafak Asar, Ş. Altındal. The investigation of frequency dependent dielectric properties and ac conductivity by impedance spectroscopy in the Al/(Cu-doped Diamond Like Carbon)/Au structures, *J. Mater. Sci: Mater. Electron.* 34, 1118, 2023. <https://doi.org/10.1007/s10854-023-10546-z>
- [10] Ç.Ş. Güçlü, E. Erbilten Tanrikulu, M. Ulusoy, Y. Azizian-Kalandaragh, Ş. Altındal. Frequency-dependent physical parameters, the voltage-dependent profile of surface traps, and their lifetime of Au/(ZnCdS-GO:PVP)/n-Si

- structures by using the conductance method, *J. Mater. Sci.: Mater. Electron.* 35, 348 (2024) <https://doi.org/10.1007/s10854-024-12111-8>
- [11] A. Abidinov, I. Afandiyeva, E. Bakhtiyarli, S. Altındal Yerişkin, S.A. Hameed. Comprehensive Investigation of Negative Capacitance and Inductive Behavior in Pure and 3% and 5% Ni-Doped PVP-Based Au/n-Si (MS) Schottky Diodes (SDs), *ACS Applied Electronic Materials* 7 (20) (2025) 9399–9407, <https://doi.org/10.1021/acsaelm.5c01377>
- [12] I.M. Afandiyeva, E.R. Bakhtiyarli, S. Altındal Yerişkin, S.A. Hameed. Negative dielectric and inductive behavior in Au/n-Si diodes with Ni-doped PVP interlayers, *Journal of Materials Science: Materials in Electronics* 2026, <https://doi.org/10.1007/s10854-026-16574-9>
- [13] A.M. Akbaş, A. Tataroğlu, Ş. Altındal, Y. Azizian-Kalandaragh. Frequency dependence of the dielectric properties of Au/(NG:PVP)/n-Si structures, *Journal of Materials Science: Materials in Electronics* 32, 7657–7670 (2021) <https://doi.org/10.1007/s10854-021-05482-9>
- [14] G.B. Parravicini, A. Stella, M.C. Ungureanu, R. Kofman. Low-frequency negative capacitance effect in systems of metallic nanoparticles embedded in dielectric matrix, *Applied Physics Letters* 85 (2) (2004) 302–304, <https://doi.org/10.1063/1.1771830>
- [15] I.Yu. Prosanov, N.F. Uvarov. Electrical properties of dehydrated polyvinyl alcohol, *Physics of the Solid State* 54 (2) (2012) 421–424, <https://doi.org/10.1134/S1063783412020278>
- [16] Ç.Ş. Güçlü, A. Khalkhali, S.A. Hameed, İ. Taşcıoğlu, A. Demirci, Ş. Altındal. Dielectric response of Au/(Co:PVA)/n-Si/Al structures under varying frequencies and bias voltages, *Journal of Materials Science: Materials in Electronics* 36 (23) (2025) 1431, <https://doi.org/10.1007/s10854-025-15485-5>
- [17] E.E. Tanrıku, S. Demirezen, Ş. Altındal, İ. Uslu. *Journal of Materials Science: Materials in Electronics* 29 (4) (2018) 2890–2898, <https://doi.org/10.1007/s10854-017-8219-1>
- [18] J.A. Fedotova, A.V. Pashkevich, A.A. Ronassi, T.N. Koltunowicz, A.K. Fedotov, P. Żukowski, A.S. Fedotov. Negative capacitance of nanocomposites with CoFeZr nanoparticles embedded into silica matrix, *Journal of Magnetism and Magnetic Materials* 511 (2020) 166963, <https://doi.org/10.1016/j.jmmm.2020.166963>
- [19] G. Fan, Z. Wang, Z. Wei, Y. Liu, R. Fan. Negative dielectric permittivity and high-frequency diamagnetic responses of percolated nickel/rutile cermet, *Composites Part A: Applied Science and Manufacturing* 139 (2020) 106132, <https://doi.org/10.1016/j.compositesa.2020.106132>
- [20] H. Biederman. Metal doped polymer films prepared by plasma polymerization and their potential applications, *Vacuum* 34 (1984) 405–410, [https://doi.org/10.1016/0042-207X\(84\)90075-7](https://doi.org/10.1016/0042-207X(84)90075-7)
- [21] G.K. Meenatchi, G. Velraj. Synthesis and characterisation of nickel oxide-carboxylated multiwalled carbon nanotube polymer nanocomposites, *Journal of Materials Science: Materials in Electronics* 34 (23) (2023) 1686, <https://doi.org/10.1007/s10854-023-10234-5>
- [22] Z. Liang, H. H. Choi, X. Luo, T. Liu, A. Abtahi, U. S. Ramasamy, J. A. Hitron, K. N. Baustert, J. L. Hempel, A. M. Boehm, A. Ansary, D.R. Strachan, J. Mei, C. Risko, V. Podzorov, K.R. Graham. n-type charge transport in heavily p-doped polymers, *Nature Materials* 20 (4) (2021) 518–524, <https://doi.org/10.1038/s41563-020-00859-3>
- [23] M. Bulinski. Metal doped PVA films for optoelectronics—optical and electronic properties, an overview, *Molecules* 26 (10) (2021) 2886, <https://doi.org/10.3390/molecules26102886>
- [24] G. Cárdenas-Triviño, N. Linares-Bermúdez, L. Vergara-González, G. Cabello-Guzmán, J. Ojeda-Oyarzún, M. Nuñez-Decape, R. Arrué-Muñoz. Synthesis and wound healing properties of polyvinyl alcohol films doped with metal nanoparticles of Cu and Ag, *Journal of the Chilean Chemical Society* 67 (4) (2022) 5667–5674, <https://doi.org/10.4067/S0717-97072022000405667>
- [25] M.H. Al-Dharob, A. Kökce, D.A. Aldemir, A.F. Özdemir, Ş. Altındal. The origin of anomalous peak and negative capacitance on dielectric behavior in the accumulation region in Au/(0.07 Zn-doped polyvinyl alcohol)/n-4H-SiC metal–polymer–semiconductor structures/diodes studied by temperature-dependent impedance measurements, *Journal of Physics and Chemistry of Solids* 144 (2020) 109523, <https://doi.org/10.1016/j.jpcs.2020.109523>
- [26] Ç. Bilkan, Y. Azizian-Kalandaragh, Ş. Altındal, R. Shokrani-Havigh. Frequency and voltage dependence dielectric properties, ac electrical conductivity and electric modulus profiles in Al/Co₃O₄-PVA/p-Si structures, *Physica B: Condensed Matter* 500 (2016) 154–160, <https://doi.org/10.1016/j.physb.2016.08.001>
- [27] A.V. Larkin, I.A. Svito, Y.A. Fedotova, A.K. Fedotov. DC and AC conductivity of metal-dielectric film nanocomposites, *Bulletin of the Belarusian State University. Ser. 1, Physics. Mathematics. Computer Science*, 2009. 1, 26.-37.
- [28] N.W. Ashcroft., N.D. Mermin. *Solid state Physics*. Harcourt College Publishers, 1976.

Received: 16.02.2026